

# Impact of gradual vascular deformations on the intra-aneurysmal hemodynamics

Samuel Voß<sup>1,2</sup>, Patrick Saalfeld<sup>3</sup>, Sylvia Saalfeld<sup>1,3</sup>, Oliver Beuing<sup>1,4</sup>,  
Gabor Janiga<sup>1,2</sup>, Bernhard Preim<sup>1,3</sup>

<sup>1</sup>STIMULATE Research Campus, University of Magdeburg

<sup>2</sup>Department of Fluid Dynamics and Technical Flows, University of Magdeburg

<sup>3</sup>Department of Simulation and Graphics, University of Magdeburg

<sup>4</sup>Institute of Neuroradiology, University Hospital Magdeburg

samuel.voss@ovgu.de

**Abstract.** The treatment of intracranial aneurysms based on stent-assisted coiling often leads to local vascular deformations. Patient-specific data of an aneurysm in the pre interventional and follow-up state is used to interpolate intermediate vessel-aneurysm configurations. Computational Fluid Dynamics simulations are performed in order to quantify the effect of vessel deformation on the blood flow. Results reveal gradual changes in the blood flow patterns shifting the load on the aneurysm wall from the dome to the neck region. Based on this novel concept, it is possible to virtually evaluate how different types of stents can improve or impair the treatment goal of reducing the intra-aneurysmal blood flow.

## 1 Introduction

Stent-assisted coiling therapy has become an established treatment strategy to prevent intracranial aneurysm rupture in order to avoid subarachnoid hemorrhage associated with severe clinical outcome. Within the endovascular treatment process, a stent is placed in front of the aneurysm. This stabilizes the parent artery and later prevents the coils from leaving the aneurysm through the aneurysms ostium, i.e., the aneurysm neck.

However, the placement of stents can cause local modifications of the vasculature (e.g., [1,2] or see Fig. 1 left and right). Furthermore, this deformation depends on the aneurysm location [1,2] and the stent design [1].

In order to evaluate the effect of the observed vascular deformation on the intra-aneurysmal hemodynamics, Computational Fluid Dynamics (CFD) can be performed. Gao et al. [3,4] virtually removed the aneurysms in pre and post interventional datasets and investigated the hemodynamic effects. Thus, significant alteration of the flow at the bifurcation apex was found, including a narrowing and migration of the flow impingement zone. Jeong et al. [5] did not exclude the aneurysm in their study but only considered simplified artificial vasculature models. In addition, effects of a stent and simplified coils were included. Hence, the vessel straightening leads to reduced values of velocity, kinetic energy, wall shear stress (WSS), and vorticity.

In a recent study from Voß et al. [6], the investigations were extended by combining 1) a patient-specific anatomy with 2) retaining the aneurysm itself. CFD analysis leads to the conclusion that vessel straightening causes a blood flow redirection resulting in a decreased aneurysm neck inflow rate.

Within the present study, we examine the intermediate states of the vascular deformation based on geometrical interpolation. For the clinical practice, this can be interpreted as employment of different stent types associated with different bending stiffnesses. By determining the gradual effect on hemodynamics, we expect a better understanding of the relation between local deformation and flow patterns. First, the progress of change of the time-dependent simulated blood flow induced by the stent can be examined. Second, important information can be virtually gathered concerning the required stent stiffness, which could support clinicians in treatment planning.

## 2 Material and Methods

### 2.1 Case description and preparation

This study is based on the image data of a 62 year old intracranial aneurysm patient. The patient was successfully treated with stent-assisted coiling therapy. Since follow-up image data revealed anatomical deformations of the parent artery harboring the aneurysm, an analysis of the pre, post and intermediate configurations was required to examine the deformation-induced changes in internal blood flow. This work extends the study presented in [6], where pre and post stent configurations but no intermediate deformations were compared.

### 2.2 Geometrical interpolation of intermediate configurations

Obtaining intermediate states between the pre and post configuration is difficult since both meshes were segmented independently and their topologies (number of vertices and their connectivity) differ. To align both topologies an approach from character modeling named *conforming* is used with the modeling software 3ds Max (Autodesk, San Rafael, USA). This techniques is also used, e.g., to deform vascular structures into flattened shapes [7]. One mesh is semi-automatically mapped onto another mesh by projecting vertices along their normal direction

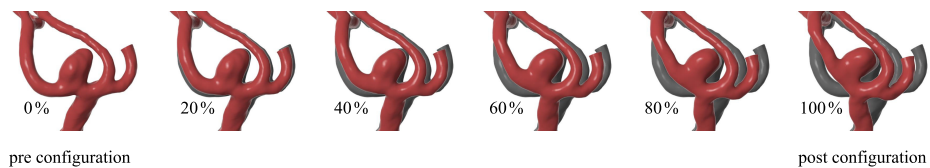


**Fig. 1.** The six configurations of our approach, 0% and 100% corresponds to the pre and post configuration, respectively.

inwards or outwards until they hit the surface of the other mesh. Doing this semi-automatically is time-consuming (approx. four hours in our case) but it allows controlling deformations and artifacts that would be produced with automatic projection approaches. Fig. 1 shows the six created states, i.e., 0%, 20%, 40%, 60%, 80%, and 100% where 0% corresponds to the pre configuration and 100% corresponds to the post configuration. The intermediate states are created with linear interpolation applied to each vertex.

### 2.3 Hemodynamic simulation

The surface meshes are imported into the simulation software STAR-CCM+ 10.04 (Siemens Product Lifecycle Management Software Inc., Plano, TX, USA) which is used to solve the Navier-Stokes equations numerically. The simulation domain is spatially discretized based on finite volume polyhedral and prism cells. An unsteady mass inflow rate is used [8]. Further, no-slip wall conditions and a flow split outlet based on the outlet area is defined. Blood is modeled as non-Newtonian fluid [6]. The CFD simulations were run on 3 nodes each with 16 cores (2x Intel Xeon E5-2630 v3). Wall-clock CPU times per case was approx. one day.

### 2.4 Extraction of morphological parameters

For an assessment of the plausibility of the intermediate interpolation steps, we analyzed the aneurysms shape based on the morphological parameters:  $S_A$  - aneurysm surface area,  $V_A$  - aneurysm volume,  $D_{Max}$  - maximum diameter parallel to ostium plane,  $H_{Max}$  - maximum distance from aneurysm to ostium,  $H_{Ortho}$  - maximum distance perpendicular to ostium plane,  $N_{Max}$  - maximum diameter of ostium, and  $AR$  - aspect ratio of the aneurysm, i.e.,  $H_{Ortho}/N_{Max}$  [9]. For the extraction of morphological parameters, we separated the aneurysm from the parent vessel with the method presented in [10]. To obtain  $V_A$  and  $S_A$ , the ostium contour is closed by connecting it with its center point. The parameter values for all datasets are provided in Tab. 1, where  $\sigma$  denotes the standard deviation and  $p_\sigma$  its percentual amount w.r.t. the mean  $\mu$ , i.e.  $p_\sigma = \sigma/\mu \cdot 100\%$ .

## 3 Results

For an evaluation of our method, we first analyzed the morphological parameter variations of the pre, post, and intermediate configurations, recall Tab. 1. As a result, we obtain very low values for  $\sigma$  indicating a high correspondence between the different configurations especially for the aneurysm's aspect ratio. Analyzing  $p_\sigma$  further confirms this finding with a maximum value of approx. 4% for the aneurysm height.

Fig. 3 indicates clear differences in the qualitative comparison of all six configurations. Due to the vascular deformation, the blood flow is redirected from the

**Table 1.** Extracted morphological parameters based on [9] for all datasets, 0 % refers to the pre, 100 % to the post configuration.

Dataset	Morphological parameters						
	$S_A$ [mm <sup>2</sup> ]	$V_A$ [mm <sup>3</sup> ]	$D_{Max}$ [mm]	$H_{Max}$ [mm]	$H_{Ortho}$ [mm]	$N_{Max}$ [mm]	$AR$
0 %	65.97	53.37	6.76	5.17	4.37	4.30	1.02
20 %	64.61	51.31	6.54	4.98	4.38	4.30	1.02
40 %	64.18	53.78	6.28	4.87	4.44	4.32	1.03
60 %	64.00	53.10	6.25	4.98	4.58	4.32	1.06
80 %	65.24	52.57	6.39	5.13	4.70	4.45	1.06
100 %	66.85	55.82	6.72	5.27	4.68	4.65	1.03
$\sigma$	1.11	1.49	0.22	0.15	0.18	0.14	0.02
$p_\sigma$	1.70 %	2.80 %	3.41 %	2.80 %	3.99 %	3.17 %	1.84 %

aneurysm dome (a) towards the neck region (f) according to streamlines (Fig. 3-1) and velocity iso-surfaces (Fig. 3-2). This change of flow patterns moves the impact zone and results in modified wall loads, represented by the time averaged wall shear stress (AWSS), see Fig. 3-3. Furthermore, the flow is more stable in the post configuration, the oscillatory shear index (OSI) decreases with increasing deformation (Fig. 3-4). This finding is supported by Fig. 2, showing more similar flow patterns over time in the post configuration. Overall, a smaller amount of blood enters the aneurysm over the cardiac cycle in the case of higher deformations, a total reduction of more than 50 % is calculated.

## 4 Discussion

The concept of intermediate states of pre interventional and follow-up aneurysm anatomy is motivated by the varying bending stiffnesses of stents in clinical use. Accordingly, this method can be used to better understand the relation between stent related vascular deformation and hemodynamics without any risk for the patient. In addition, within a semi-automatized workflow, different scenarios can be virtually compared in order to 1) assess different treatment options or devices

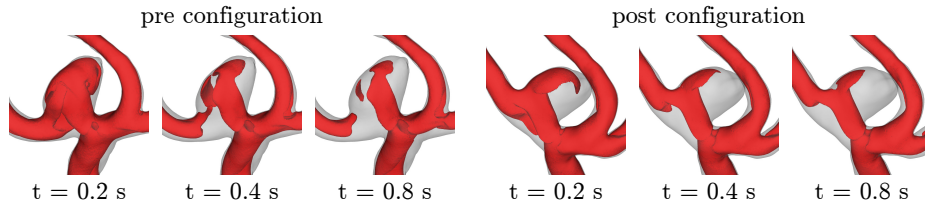


**Fig. 2.** Iso-surfaces of the velocity field at 0.5 m/s for different time steps: In the pre interventional configuration (left) the flow patterns vary over time, while in the post interventional configuration (right) the flow is rather constant.

and 2) consider possible uncertainties due to individual mechanical properties of the vessel wall, potential pathologies and surrounding structures.

Our evaluation showed errors less than 4% for morphological parameters due to the geometrical interpolation. From the computed blood flow, we observe clear differences in the inflow rates, which is important for thrombus formation and aneurysm occlusion. In our case, vascular deformation leads to changes that can be expected to have a positive effect on the clinical outcome. However, in other patients such high grades of deformation may have the opposite effect and impair the flow conditions.

**Acknowledgments.** This work is partly funded by the European Regional Development Fund under the operation number ZS /2016/04/78123 as part of the initiative Sachsen-Anhalt WISSENSCHAFT Schwerpunkte.

## References

1. Gao B, Baharoglu MI, Cohen AD, et al. Stent-assisted coiling of intracranial bifurcation aneurysms leads to immediate and delayed intracranial vascular angle remodeling. *Am J Neuroradiol.* 2012;33(4):649–654.
2. Chau Y, Mondot L, Sachet M, et al. Modification of cerebral vascular anatomy induced by Leo stent placement depending on the site of stenting: A series of 102 cases. *Interv Neuroradiol.* 2016;22(6):666–673.
3. Gao B, Baharoglu MI, Malek AM. Angular remodeling in single stent-assisted coiling displaces and attenuates the flow impingement zone at the neck of intracranial bifurcation aneurysms. *Neurosurgery.* 2013;72(5):739–748.
4. Gao B, Baharoglu MI, Cohen AD, et al. Y-stent coiling of basilar bifurcation aneurysms induces a dynamic angular vascular remodeling with alteration of the apical wall shear stress pattern. *Neurosurgery.* 2013;72(4):617–629.
5. Jeong W, Han MH, Rhee K. The hemodynamic alterations induced by the vascular angular deformation in stent-assisted coiling of bifurcation aneurysms. *Comput Biol Med.* 2014;53:1–8.
6. Voß S, Berg P, Janiga G, et al. Variability of intra-aneurysmal hemodynamics caused by stent-induced vessel deformation. *Curr Dir Biomed Eng.* 2017;3(2):305–308.
7. Saalfeld P, Glaßer S, Beuing O, et al. The FAUST framework: Free-form annotations on unfolding vascular structures for treatment planning. *Comput Graph.* 2017;65:12–21.
8. Berg P, Stucht D, Janiga G, et al. Cerebral blood flow in a healthy circle of willis and two intracranial aneurysms: computational fluid dynamics versus four-dimensional phase-contrast magnetic resonance imaging. *J Biomech Eng.* 2014;136(4):041003/1–9.
9. Lauric A, Baharoglu MI, Malek AM. Ruptured status discrimination performance of aspect ratio, height/width, and bottleneck factor is highly dependent on aneurysm sizing methodology. *Neurosurgery.* 2012;71(1):38–46.
10. Neugebauer M, Diehl V, Skalej M, et al. Geometric reconstruction of the ostium of cerebral aneurysms. *Proc Vision, Modeling, and Visualization.* 2010; p. 307–314.

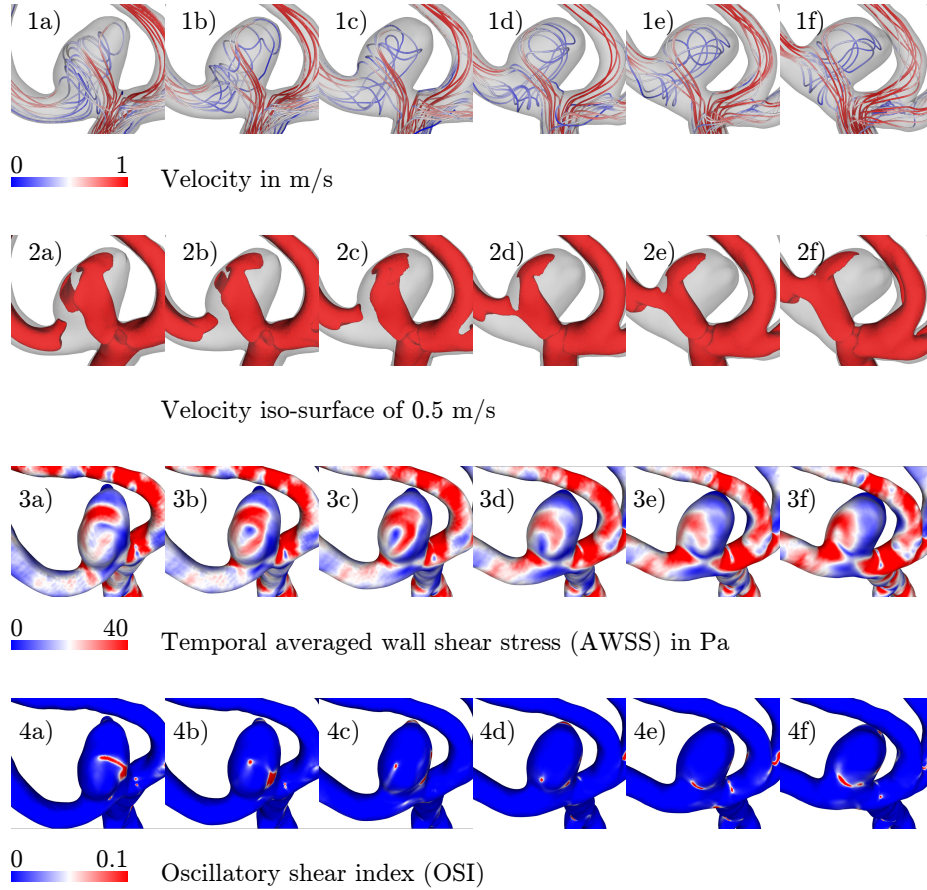


**Fig. 3.** The different deformation configurations are shown from the pre (a) to the post (f) interventional state from left to right, respectively. First row: The deformation affects the intra-aneurysmal blood flow, visualized using velocity-coded streamlines of the time averaged flow field. Second row: Iso-surfaces of the velocity field at 0.5 m/s show a gradual migration of the flow impingement zone from the aneurysm dome (a) towards the neck region (f). This redirection of the blood flow is caused only by changes of the local vasculature. Third row: Local time averaged wall shear stress (AWSS) values vary according to the redirected blood flow. While the more pre configurations (a) to (c) show higher values at the aneurysm dome, in the more post configurations (d) to (f) values are higher in the neck region. Fourth row: Vascular deformations cause considerable changes in the oscillatory shear index (OSI). High values in configurations (a) and (b) indicate fluctuations in the time dependent flow patterns.